PHYSICAL REVIEW D VOLUME 51, NUMBER 11 1 JUNE 1995

# Electric dipole moment of the $W$ boson in the two-Higgs-doublet extension of the standard model

Rafael López-Mobilia* and Todd H. West†
*Theory Group, Department of Physics, University of Texas at Austin, Austin, Texas 78712*
(Received 30 June 1994)

We compute the electric dipole moment (EDM) of the $W$ boson in the two-Higgs-doublet extension of the standard model. The calculation is performed at two loops with all the relevant Feynman diagrams included. We find that the $W$-boson EDM may be as large as $10^{-21} - 10^{-20} e$ cm, for reasonable masses of the top quark and Higgs boson. Our results disagree with previous calculations done by He and McKellar and Vendramin.

PACS number(s): 11.30.Er, 12.38.Bx, 12.60.Fr, 13.40.Gp

## I. INTRODUCTION

Electric dipole moments (EDM's) of elementary particles have become an important area of speculation in the ongoing search for an explanation of the still mysterious phenomenon of $CP$ violation. Its appeal comes from two observations. First, the *reality* of $CP$ violation in nature (the neutral kaon system is the only place in which it has been observed) suggests that all non-self-conjugated particles may possess EDM's, albeit small ones. Second, the standard model (SM) can accommodate $CP$-violating interactions by means of the Kobayashi-Maskawa mechanism (through a *single* phase for three generations of quarks), but the predicted EDM's are extremely small. Yet, this is not so in many interesting extensions of the SM (such as multi-Higgs models, supersymmetry, etc.) which include, for the most part, a plethora of additional $CP$-violating phases and tend to produce much stronger $CP$-violating effects [1].

The advantage of studying EDM's is then twofold. We can restrict, in some cases, the parameter space of a theory by comparing the predicted values with experimental upper bounds. On the other hand, if an (elementary particle) EDM is observed, that would almost surely signal physics beyond the SM.

Among the SM particles, most of the interest has been centered on the neutron and the electron [2], because of the relative ease with which tight EDM bounds can be established in low energy experiments. By contrast, particles such as the $W$ boson require the analysis of $CP$-odd asymmetries in high energy processes and good bounds may be hard to come by. Still, given the increasing energies and luminosities of current and proposed accelerators it may be possible in the near future to supply stronger constraints on the EDM of the $W$ boson (for investigations on these matters, see Refs. [3] and [4]). Furthermore, starting with the work of Marciano and Queijeiro [5] it has become clear that a $W$-boson EDM can induce large fermion EDM's and in some theories the dominant contribution to the electron EDM may come from this mechanism. For instance, this seems to be the case in the SM [6].

The importance of studying the properties of a nonminimal Higgs sector cannot be overstressed, in view of its potential richness and the fact that we still do not know if the simplest (i.e., one-Higgs-doublet in the minimal SM) version is the one chosen by nature.

The current interest in EDM's arising from ($CP$-violating) Higgs-boson exchange was initiated, to a large extent, a few years ago by the papers of Weinberg [7,8]. In [7] he showed that neutral-Higgs-boson exchange could induce a very large neutron EDM, through a class of Feynman diagrams previously neglected. Inspired by this, Barr and Zee [9] found another class of graphs (at the two-loop level) which turned out to give the dominant contribution to the EDM of the electron, several orders of magnitude above the one-loop result.

The upper bound, $d_W \lesssim 10^{-19}$ e cm, for the $W$ EDM comes from the experimental upper bound for the neutron EDM [$d_n = (-3 \pm 5) \times 10^{-26}$ e cm [10]] after applying the Marciano-Queijeiro method of computing the induced fermion EDM's. This is not a direct measurement and should be taken with reservations since the calculation, although model independent, involves many uncertainties [11] (additional comments in the conclusions of this paper). The $W$ EDM predicted by the SM has been estimated to be no larger than about $10^{-29}$ e cm [6]. By contrast, we find that in the two-Higgs-doublet model its value may be as large as $10^{-21} - 10^{-20}$ e cm, for reasonable masses of the top quark and neutral Higgs boson and without overstretching the values of the $CP$-violating phases that enter the calculation. He and McKellar [12] and Vendramin [13] computed in detail one of the diagrams [see Fig. 1(a)] but our calculations contradict both. Our result is *larger* than that of He and McKellar and *smaller* than Vendramin's, in both cases by about an order of magnitude. We contacted He and McKellar on this issue and they revised their calculations. They now agree with our results for this diagram and have published an

*Electronic address: rafael@utaphy.ph.utexas.edu
†Electronic address: toddwest@utaphy.ph.utexas.edu

 

erratum [14].

Chang *et al.* [15] made an estimate that has too strong a dependence on the neutral-Higgs-boson mass. For more details see the conclusions at the end of this paper.

This paper is organized as follows. In Sec. II we introduce some notation and definitions, paying particular attention to a description of those aspects of the two-Higgs-doublet model relevant to our calculation. In Sec. III we discuss the Feynman diagrams that give contributions to the $W$ EDM at the two loop level, deferring a discussion of those that do not contribute to the Appendix. Then we move (Sec. IV) to the analysis of the calculations themselves, giving the concluding remarks in Sec. V.

## II. DISCUSSION OF MODEL AND NOTATION

The possession, by an elementary particle, of an electric dipole moment violates both parity ($P$) and time reversal ($T$) symmetries [16]. This is the only $(P,T)$-violating moment that a spin-$\frac{1}{2}$ particle can possess. However we find additional $(P,T)$-violating moments as we move to higher spins. A spin-1 particle (such as the $W$ boson) can have one more $P$ and $T$ odd moment, the magnetic quadrupole (MQM) in addition to the EDM. It may also carry a $CP$-violating (but $P$ conserving) moment [3]. In this work we confine ourselves to the EDM and MQM.

The matrix element of the electromagnetic current $J^\mu$, between identical initial and final one-particle states, can be decomposed into a linear combination of form factors. For a $W$ boson (spin-1) this matrix element is [17,18]

$$\langle W|J^\mu|W\rangle = -ie\varepsilon^*_\sigma(p_2)\Gamma^{\sigma\nu\mu}(p_1,p_2)\varepsilon_\nu(p_1)\ , \tag{1}$$

where the $(P,T)$-violating piece of the tensor $\Gamma$ is

$$\Gamma^{\sigma\nu\mu}_{(P,T)\ \text{odd}} = -f_\gamma(q^2)\varepsilon^{\sigma\nu\mu\rho}q_\rho - \frac{1}{m_W^2}g_\gamma(q^2)p^\mu\varepsilon^{\sigma\nu\rho\tau}q_\rho p_\tau\ . \tag{2}$$

The notation is as follows: $p_1$ and $p_2$ are the initial and final four-momenta of the $W$ boson, respectively; the $\varepsilon_\mu(p_i)$'s are the polarization vectors; $q \equiv p_1 - p_2$ and $p \equiv p_1 + p_2$; and the form factors $f_\gamma(q^2)$ and $g_\gamma(q^2)$ are related to the $W$ boson EDM ($d_W$) and MQM ($\tilde{Q}_W$) through

$$d_W = \frac{e}{2m_W}\{f_\gamma(0) - 4g_\gamma(0)\}\ , \tag{3}$$

$$\tilde{Q}_W = -\frac{e}{m_W^2}f_\gamma(0)\ . \tag{4}$$

We shall work in the two-Higgs-doublet extension of the standard model [8]. In this theory the SU(2)×U(1) electroweak symmetry is broken by two Higgs doublets. In order to avoid excessive rates of flavor-changing neutral current processes we will allow one of the doublets to couple to the up-type quarks only and the other to the down-type quarks (the so-called model II scheme [19]). This can be achieved by imposing a discrete symmetry enforcing the aforementioned couplings, but in a renormalizable Lagrangian such an exact symmetry rules out $CP$ violation and therefore has to be softly broken.

Let

$$\phi_k \equiv \begin{pmatrix} \phi_k^+ \\ \phi_k^0 \end{pmatrix}, \quad \text{where } k = \{1,2\}\ , \tag{5}$$

be the scalars that couple to the quarks, with vacuum expectation values $\lambda_k \equiv \langle\phi_k^0\rangle_{\text{vac}}$, $k = \{1,2\}$. Then, the Yukawa sector of the Lagrangian is given by

$$\mathcal{L}_Y = -\frac{1}{\lambda_2}\bar{U}_R m_U U_L \phi_2^0 - \frac{1}{\lambda_1^*}\bar{D}_R m_D D_L \phi_1^{0*} - \frac{1}{\lambda_1^*}\bar{D}_R m_D V^\dagger U_L \phi_1^{+*} + \frac{1}{\lambda_2}\bar{U}_R m_U V D_L \phi_2^+ + \text{H.c.}\ , \tag{6}$$

where $U$ and $D$ are the up- and down-type quark triplets, respectively, with $m_U$ and $m_D$ the diagonal mass matrices. $V$ is the Kobayashi-Maskawa matrix. (We will assume $V_{tb} = 1$, for simplicity.)

The unphysical Goldstone bosons and the charged Higgs bosons are defined as

$$G^+ = \frac{1}{R}(\lambda_1^*\phi_1^+ + \lambda_2^*\phi_2^+),\quad G^0 = \frac{\sqrt{2}}{R}\text{Im}(\lambda_1^*\phi_1^0 + \lambda_2^*\phi_2^0) \tag{7}$$

and

$$H^+ = \frac{1}{R}(\lambda_1\phi_2^+ - \lambda_2\phi_1^+)\ , \tag{8}$$

respectively, where $R \equiv \sqrt{|\lambda_1|^2 + |\lambda_2|^2}$. To simplify the notation we shall define, as has become usual, $\tan\beta = |\lambda_2/\lambda_1|$. The Fermi coupling constant is given by $2\sqrt{2}G_F = (|\lambda_1|^2 + |\lambda_2|^2)^{-1}$, where a factor of 2, missing in Ref. [8], is included.

The "propagators" for the scalars are defined by

$$\langle\eta\xi\rangle_q \equiv \int d^4x\langle 0|T\{\eta(x)\xi(0)\}|0\rangle e^{iq\cdot x} \tag{9}$$

and, following Weinberg, we write

$$\langle\phi_2^0\phi_2^0\rangle_q \equiv -(\lambda_2)^2\sum_n \frac{\sqrt{2}G_F Z_{2,n}}{q^2 - m_{Hn}^2} \approx -\frac{\sqrt{2}G_F(\lambda_2)^2 Z_2}{q^2 - m_H^2}\ , \tag{10}$$

$$\langle\phi_2^0\phi_1^0\rangle_q \equiv -\lambda_1\lambda_2\sum_n \frac{\sqrt{2}G_F\tilde{Z}_{0,n}}{q^2 - m_{Hn}^2} \approx -\frac{\sqrt{2}G_F\lambda_1\lambda_2\tilde{Z}_0}{q^2 - m_H^2}\ , \tag{11}$$

$$\langle\phi_2^0\phi_1^{0*}\rangle_q \equiv -\lambda_1^*\lambda_2\sum_n \frac{\sqrt{2}G_F Z_{0,n}}{q^2 - m_{Hn}^2} \approx -\frac{\sqrt{2}G_F\lambda_1^*\lambda_2 Z_0}{q^2 - m_H^2}\ , \tag{12}$$

$$\langle \phi_1^0 \phi_1^0 \rangle_q \equiv -(\lambda_1)^2 \sum_n \frac{\sqrt{2} G_F Z_{1,n}}{q^2 - m_{Hn}^2} \approx -\frac{\sqrt{2} G_F (\lambda_1)^2 Z_1}{q^2 - m_H^2} \ , \tag{13}$$

where the sum is over all mass eigenstates and the expression on the right of each definition corresponds to the approximation in which one of the scalars (with mass $m_H$) dominates over the other (presumably) more massive ones. (We will employ this assumption in what follows.) $G_F$ is the Fermi constant. The dimensionless coefficients $Z_1, Z_2, Z_0$, and $\tilde{Z}_0$ are in general complex, and $CP$ violation will show up if they possess (nonzero) imaginary parts. The corresponding propagator for charged Higgs bosons is real in the two-Higgs-doublet case, and so there is no $CP$ violation in the exchange of charged scalars. However, diagrams with neutral Higgs bosons *and* charged Higgs bosons do violate, in general, $CP$ invariance. Given that the inclusion of those diagrams introduces one more unknown parameter in the calculations and does not appreciably affect our conclusions, we shall disregard them in what follows, with the exception of an important subtlety examined in Sec. IV. We will also employ the following relation between the $CP$-violating amplitudes,

$$|\lambda_2|^2 \mathrm{Im} Z_2 + |\lambda_1|^2 \mathrm{Im} \tilde{Z}_0 = |\lambda_1|^2 \mathrm{Im} Z_0 \ , \tag{14}$$

which is a direct consequence of the definitions for the $Z$'s and the unitarity gauge condition [8]. And finally, in order to be able to compare the contributions proportional to different $Z_i$'s, we make use of the bounds found by Weinberg:

$$|\mathrm{Im} Z_0| \leq \frac{1}{2}(|\lambda_1/\lambda_2| + |\lambda_2/\lambda_1|) \ , \tag{15}$$

$$|\mathrm{Im} \tilde{Z}_0| \leq \frac{1}{2}(|\lambda_1/\lambda_2| + |\lambda_2/\lambda_1|) \ , \tag{16}$$

$$|\mathrm{Im} Z_2| \leq (|\lambda_1/\lambda_2|^2 + |\lambda_1/\lambda_2|^4)^{1/2} \ . \tag{17}$$

(A missing factor of 2 in Ref. [8] has been corrected.) These expressions give an upper bound of order unity to $\mathrm{Im} Z_2$, $\mathrm{Im} Z_0$, and $\mathrm{Im} \tilde{Z}_0$, when $\lambda_1$ and $\lambda_2$ are of the same order of magnitude. The same is true of the quantity $2 \cos^2 \beta \mathrm{Im} Z_0$ that shows up in the calculation of many of our diagrams.

## III. DIAGRAMS

The dominant contributions to the EDM of the $W$ boson come, in the two-Higgs-doublet model, from two-loop diagrams. In order to generate a Levi-Civita tensor (to violate $P$ invariance) a fermion loop is required and in addition at least one neutral Higgs propagator insertion is needed to violate $CP$ invariance. These two conditions are impossible to satisfy at less than two loops. At this level the number of potentially contributing diagrams is rather large (in the hundreds), but a careful analysis reduces it to a manageable size. For a given diagram there are several possible neutral Higgs propagator insertions [see Eqs. (10)–(13)], according to the admissible couplings in the theory. For instance, there is no coupling of $\phi_1^0$ to the top quark and consequently the only possible insertions in diagram (a) of Fig. 1 are $\langle \phi_2^0 \phi_2^0 \rangle$ and $\langle \phi_2^{0*} \phi_2^{0*} \rangle$. In other cases there may be up to six different neutral Higgs propagator insertions. (Each one corresponds essentially to a different diagram.)

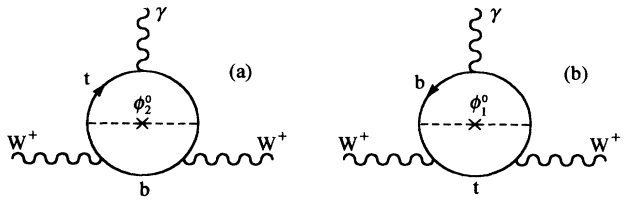


FIG. 1. Class 1 diagrams (see Sec. III). The diagrams shown are the only ones in this class and they both contribute to the EDM of the $W$ boson. However 1(b) is strongly suppressed relative to 1(a) by the couplings of the bottom quark to the Higgs boson.

We have divided the contributing diagrams into classes labeled 1 through 4 (see Figs. 1–4), according to how the external $W$ bosons and internal scalar propagators are attached to the fermion loop. Classes 1 and 2 have *both* external $W$'s directly connected to the quark loop. Class 3 has one external $W$ attached to it. In class 4 no external $W$'s touch the loop. In all cases (the ones that produce $P$ and $CP$ violation) the neutral Higgs propagator is attached to the fermion loop.

In class 1 there are only two diagrams. Only 1(a) [Fig. 1(a)] gives a sizable contribution (proportional to $\mathrm{Im} Z_2$) since 1(b) is strongly suppressed relative to 1(a) by a factor of $(m_b/m_t)^2$.

Class 2 diagrams (in Fig. 2 we show only a few of them to illustrate their topology) are again small relative to 1(a) because of the presence of a bottom-quark–neutral-Higgs-boson coupling. Moreover, the suppression in these diagrams is also of order $(m_b/m_t)^2$ since two top-quark mass factors get replaced by bottom masses, one from the couplings to the scalars and the other from the traces.

Class 3 (Fig. 3) contains, naively, 36 diagrams plus an equal number of symmetric ones, with identical contributions, in which the neutral Higgs propagators are attached to the incoming $W$ boson. Since we are working

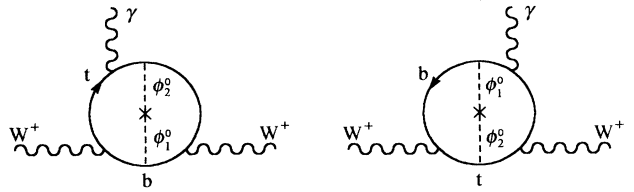


FIG. 2. Class 2 diagrams (see Sec. III). Only two of them are shown (out of 16, if all possible scalar propagator insertions and photon attachments are considered). These diagrams are also suppressed relative to 1(a).

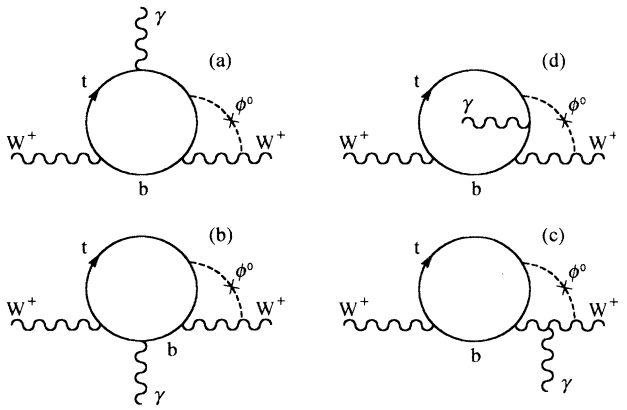


FIG. 3. Class 3 diagrams (see Sec. III). Only the four main topologies are shown. To these, we need to add diagrams with unphysical Goldstone bosons in place of the internal $W$ bosons and symmetric diagrams in which the neutral Higgs boson is attached to the incoming $W$ boson. In each case, several different neutral Higgs propagator insertions are possible (6 for internal $W$ diagrams and 4 for Goldstone boson diagrams).

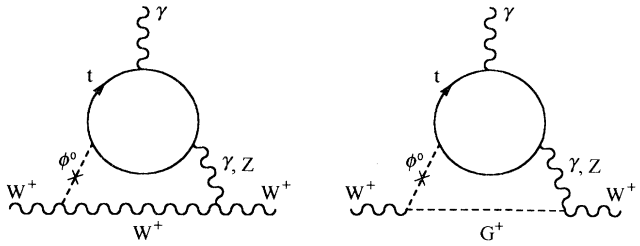


FIG. 4. Class 4 diagrams (see Sec. III). "Barr-Zee"-like diagrams with internal photon or $Z^0$ particle. Diagrams with the top loop flow reversed and symmetric diagrams with the neutral Higgs boson connected to the outgoing $W$ boson are part of this set. Those graphs in which the $Z^0$ is replaced with an unphysical neutral Goldstone boson do not contribute.

in the 't Hooft–Feynman gauge, diagrams with unphysical Goldstone bosons have to be included in order to get a gauge invariant result. A careful analysis of the diagrams shows that most of them can be computed from a set of just nine different parametric integrals. This excludes diagrams with charged Higgs bosons (more on this later). All their contributions are comparable to that of diagram 1(a), barring the fact that they are proportional to the quantity $\cos^2\beta \mathrm{Im} Z_0$ (as we show later), not $\mathrm{Im} Z_2$.

Finally, class 4 (see Fig. 4) contains diagrams with internal $W$ bosons and photons or $Z^0$ bosons and related diagrams with unphysical Goldstone bosons. Diagrams with the top-quark running in the opposite direction and diagrams with the scalar propagator attached to the outgoing $W$ boson produce the same contributions. (Note that crossing the legs of the fermion loop is equivalent to reversing its flow together with switching the attachment of the scalar from one external $W$ boson to the other one.) Again, naively, the total number of diagrams to be computed is large ($> 100$), but everything can be reduced to the evaluation of only two parametric integrals. Their contributions are, once more, comparable in magnitude to that coming from the diagram of Fig. 1(a) and proportional, as in class 3, to $\cos^2\beta \mathrm{Im} Z_0$.

In Fig. 7 we give a few examples of diagrams that *do not* contribute to the EDM of the $W$ boson. The explanation is relegated to the Appendix.

## IV. CALCULATIONS

For each diagram there are several possible contributions depending on what scalar propagator insertions are acceptable. All such contributions must be summed and from the resulting total amplitude we pick those pieces proportional to the imaginary part of the neutral Higgs propagators (to violate $CP$) and containing a Levi-Civita tensor (to violate $P$). We can then look for the coefficients of the specific tensor structures corresponding to the form factors of Eq. (2). This task is simplified if we express from the start all quantities in terms of the independent momenta $p = p_1 + p_2$ and $q = p_1 - p_2$, where $p_1$ and $p_2$ are the momenta of the incoming and outgoing $W$ bosons, respectively.

It is worth mentioning that we have made use of programs we wrote in MATHEMATICA [20] to symbolically perform the traces of Dirac $\gamma$ matrices and convert the momentum integrals into integrals over Feynman parameters [21]. The final numerical multidimensional integrations were done with MATHEMATICA's own algorithms.

For diagram 1(a) [Fig. 1(a)] the tensor amplitude $\Gamma^{\sigma\nu\mu}_{T\,\mathrm{odd}}$ (which becomes that of Eq. (2) after selecting the $P$-odd part) is given by the integral

$$\Gamma^{\sigma\nu\mu}_{T\,\mathrm{odd}} = \frac{1}{16} G_F \sqrt{2} g^2 m_W^2 \mathrm{Im} Z_2 (m_t/m_W)^2 \int \frac{d^4k}{(2\pi)^4} \frac{d^4l}{(2\pi)^4} \frac{i(T^{(1)} - T^{(2)})^{\sigma\nu\mu}}{D} , \tag{18}$$

where

$$\begin{aligned} T^{(1)}_{\sigma\nu\mu} = \mathrm{Tr}[&\gamma_\nu(1-\gamma_5)(\not{l} - \not{p}/2 + m_b)\gamma_\sigma(1-\gamma_5)(\not{l} - \not{q}/2 + m_t)(1+\gamma_5) \\ &\times(\not{k} - \not{q}/2 + m_t)\gamma_\mu(\not{k} + \not{q}/2 + m_t)(1+\gamma_5)(\not{l} + \not{q}/2 + m_t)] , \end{aligned} \tag{19}$$

$$T^{(2)}_{\sigma\nu\mu} = \mathrm{Tr}[\gamma_\nu(1-\gamma_5)(\not{l} - \not{p}/2 + m_b)\gamma_\sigma(1-\gamma_5)(\not{l} - \not{q}/2 + m_t)(1-\gamma_5) \times(\not{k} - \not{q}/2 + m_t)\gamma_\mu(\not{k} + \not{q}/2 + m_t)(1-\gamma_5)(\not{l} + \not{q}/2 + m_t)] \tag{20}$$

and the denominator

$$D = \left[\left(l - \frac{1}{2}p\right)^2 - m_b^2\right]\left[\left(l - \frac{1}{2}q\right)^2 - m_t^2\right]\left[\left(l + \frac{1}{2}q\right)^2 - m_t^2\right] \times\left[\left(k - \frac{1}{2}q\right)^2 - m_t^2\right]\left[\left(k + \frac{1}{2}q\right)^2 - m_t^2\right][(l-k)^2 - m_H^2] \, . \tag{21}$$

In these equations, $q = p_1 - p_2$ is the momentum of the photon and $p = p_1 + p_2$ is the sum of the momenta of the external $W$'s. The other parameters are self-explanatory and a factor of 3 (for the quark colors) is already included in Eq. (18). In this particular diagram, we can make $q = 0$ in $D$, since after the evaluation of the traces (before integration) every ($P$-odd) term contains at least one power of $q$ and that is all we need in order to compute $f_\gamma(0)$ and $g_\gamma(0)$. This reduces the number of terms in the denominator from 6 to 4 which, in turn, simplifies the final parametric form. For other diagrams this is, in general, not true and the number of Feynman parameters is in consequence larger.

Performing the traces and selecting the $P$-odd pieces, we get, from (18),

$$\Gamma^{\sigma\nu\mu}_{P,T\ \mathrm{odd}} = \frac{1}{16}G_F\sqrt{2}g^2m_W^2\mathrm{Im}Z_2(m_t/m_W)^2\int\frac{d^4k}{(2\pi)^4}\frac{d^4l}{(2\pi)^4}T^{\sigma\nu\mu}/D' \, , \tag{22}$$

where

$$T^{\sigma\nu\mu} = 32m_t^2(-2\varepsilon^{\mu\nu\sigma\alpha}l_\alpha l\cdot q + 2\varepsilon^{\nu\sigma\alpha\rho}k_\mu l_\alpha q_\rho - 2\varepsilon^{\nu\sigma\alpha\rho}l_\mu l_\alpha q_\rho - \varepsilon^{\nu\sigma\lambda\rho}k_\mu p_\lambda q_\rho + \varepsilon^{\nu\sigma\lambda\rho}l_\mu p_\lambda q_\rho) \, , \tag{23}$$

and $D'$ is $D$ from (21) with $q = 0$. After rewriting $D'$ in parametric form and doing the momenta integrations, we look for contributions to $f_\gamma$ and $g_\gamma$, according to the definition (2) and get

$$f_\gamma(0) = \frac{G_F\sqrt{2}g^2m_W^2}{128\pi^4}\mathrm{Im}Z_2F_{1a}(m_t, m_H) \, , \tag{24}$$

$$g_\gamma(0) = \frac{G_F\sqrt{2}g^2m_W^2}{128\pi^4}\mathrm{Im}Z_2G_{1a}(m_t, m_H) \, , \tag{25}$$

where the functions $F_{1a}$ and $G_{1a}$ are given by the Feynman parameter integrals

$$F_{1a}(m_t, m_H) = (m_t/m_W)^2\int_0^1 dx\int_0^1 dy\int_0^1 dz(1+x)(1-y) \times[(1-x)/y - z + x + (m_H/m_t)^2(1-x)(1-z)/x - (m_W/m_t)^2z(1-x)(1-yz)]^{-1} \, , \tag{26}$$

$$G_{1a}(m_t, m_H) = \int_0^1 dx\int_0^1 dy\int_0^1 dz(1-x)(1-y)(1-yz)(z/2x) \times[(y-1)/y + (z-1)/x + (m_W/m_t)^2z(1-yz) - (m_H/m_t)^2(y-z)/(1-x)]^{-2} \, . \tag{27}$$

In these (and future) expressions, the mass of the bottom quark is set equal to zero. The relative error introduced is typically no larger than $10^{-3}$. We have evaluated numerically these integrals for different combinations of masses. The results, converted to the EDM of the $W$ boson, are shown in the plots of Fig. 5 [curve (a) in each graph] where $\mathrm{Im}Z_2$ is taken to be equal to one. The main contributions come from $f_\gamma(0)$ and that happens to be true for all the diagrams. In fact, the values for $g_\gamma(0)$ are small, typically 10 to 100 times smaller than those for $f_\gamma(0)$. Moreover, the contributions to $g_\gamma(0)$ from diagrams with unphysical Goldstone bosons and from all class 4 diagrams are null. We will disregard $g_\gamma(0)$ in what follows and compute the EDM of the $W$ boson from $f_\gamma(0)$ alone. This together with setting the mass of the bottom quark equal to zero and the assumption of one dominant Higgs boson are the only approximations employed. Everything else is exact, to within the precision of the

numerical integrations.

We can see from the expression for $F_{1a}$ that the behavior of $d_W$ is roughly quadratic in $m_t$ and decreases as $m_H$ increases. This is expected and consistent with our assumption that the contribution from the lightest neutral-Higgs-boson mass-eigenstate is dominant. However, for large values of the mass of the top quark, the tree-level vertices of Eq. (6) will be significantly modified by higher order corrections, and therefore we cannot expect the quadratic dependence to hold [22].

The contribution from these diagrams is proportional to the quantity $\mathrm{Im}Z_2$, which can be of order one, assuming the vacuum expectation values $\lambda_1$ and $\lambda_2$ to be comparable in magnitude (see Sec. II). For the particular choice $m_t = 180$ GeV and $m_H = 100$ GeV we get $f_\gamma(0) = 1.4 \times 10^{-5}\ \mathrm{Im}Z_2$ and $g_\gamma(0) = 1.1 \times 10^{-7}\ \mathrm{Im}Z_2$, which correspond to an EDM, $d_W = 1.7 \times 10^{-21}\ \mathrm{Im}Z_2\ e$ cm. This is approximately seven times larger than the value obtained by He and McKellar [12] for this diagram. As noted in the introduction, they have checked their calculations and found some errors. Their results now agree with ours [14].

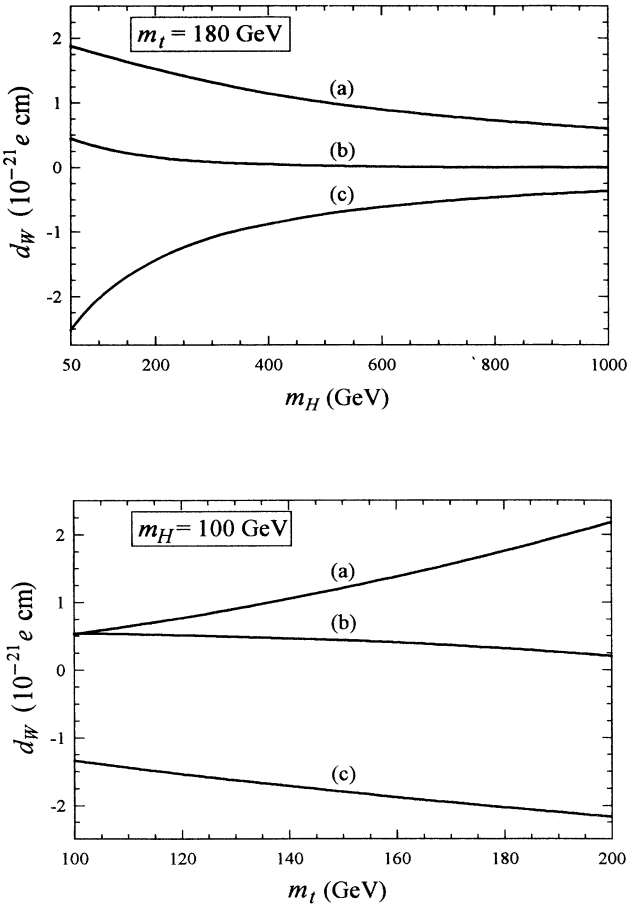


FIG. 5. Electric dipole moment of $W$ boson contributed by the different sets of diagrams, for the cases $m_t = 180$ GeV (upper plot) and $m_H = 100$ GeV (lower plot). In both plots, curve (a) shows the contribution of diagram 1(a) [see Fig. 1(a)], with $\mathrm{Im}Z_2 = 1$. Curve (b) corresponds to class 3 diagrams (see Fig. 3), with $2\cos^2\beta\mathrm{Im}Z_0 = 1$. Curve (c) is the one coming from class 4 diagrams (see Fig. 4), again with the assumption $2\cos^2\beta\mathrm{Im}Z_0 = 1$.

Class 3 diagrams are more difficult to compute. They contain internal $W$ bosons and the corresponding diagrams with unphysical Goldstone bosons. Except for some of the diagrams, the expressions for $F$ and $G$ are very complicated and the integrations are over four or five Feynman parameters. Their explicit forms are not very illuminating, but a few words are in order. Diagrams with internal $W$ bosons vary slowly with $m_t$ (or $m_H$), but diagrams 3(a),(b),(d) (see Figures) with an unphysical Goldstone boson replacing the $W$ boson behave like diagram 1(a); that is, they are approximately quadratic in $m_t$. Diagram 3(c) with Goldstone bosons is, like its parent diagram with $W$'s, slowly varying.

We also found that many Goldstone boson diagrams are divergent. This, of course, does not make sense since we are computing the lowest order contributions to the EDM of the $W$ boson in this model, and therefore they should be finite. Fortunately, the infinities cancel with infinities coming from similar diagrams with charged Higgs bosons replacing the unphysical Goldstone bosons, leaving a finite remnant (see Fig. 6). It therefore appears imperative to include those diagrams in a consistent calculation. However a new parameter would be introduced in the computations, namely, the mass of the charged Higgs boson. To avoid complicating the calculations unnecessarily, we shall ignore these finite remnants. We will also neglect the whole set of *finite* charged-Higgs diagrams. Nevertheless, it seems clear that their contributions are about the same size as those from the other diagrams, for values of the charged-Higgs-boson mass comparable to the $W$-boson mass. In fact, in the case of the divergent charged-Higgs diagrams, for a mass of the charged Higgs boson *equal* to $m_W$ the contributions are the same, but of opposite sign, as those from the corresponding diagrams with unphysical Goldstone bosons. (And hence not only do the infinite pieces cancel, but also the finite remnant becomes zero.)

All contributions from this set can be written in terms of $\mathrm{Im}Z_0$. For example, for diagram 3(a), after considering the three possible neutral Higgs propagator insertions (and their complex conjugates), we find

$$f_\gamma(0) = \frac{g^4}{32(4\pi)^4} 2\sqrt{2} G_F \times (|\lambda_2|^2 \mathrm{Im}Z_2 + |\lambda_1|^2 \mathrm{Im}\tilde{Z}_0 + |\lambda_1|^2 \mathrm{Im}Z_0) \times F_{3a}(m_t, m_H) \quad (28)$$

$$= \frac{g^4}{32(4\pi)^4} (2\cos^2\beta \mathrm{Im}Z_0) F_{3a}(m_t, m_H) \quad (29)$$

after applying the identity (14). For the same combination of masses as before, $m_t = 180$ GeV and $m_H = 100$ GeV, we get $f_\gamma(0) = 1.2 \times 10^{-6}(2\cos^2\beta\mathrm{Im}Z_0)$. All diagrams in this set contribute roughly the same (in magnitude) and there is partial cancellation among some of them. Adding all diagrams and multiplying by 2 (in order to include the symmetric diagrams mentioned in the previous section) we find $f_\gamma(0) = 2.6 \times 10^{-6}(2\cos^2\beta\mathrm{Im}Z_0)$, for the above masses of the top quark and the neutral Higgs boson. The EDM coming from this and other com-

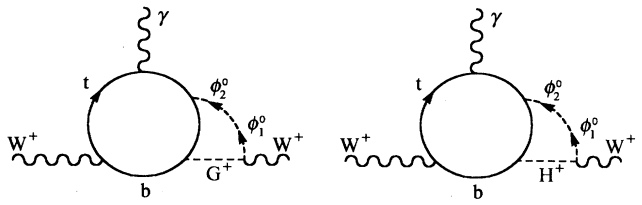


FIG. 6. An example of divergent diagrams whose infinities cancel mutually, leaving a finite residue. (See Sec. IV). The one on the left has an unphysical Goldstone boson and the other a charged Higgs boson. The diagrams cancel altogether when the mass of the charged Higgs boson is equal to the $W$-boson mass.

binations of masses is depicted in Fig. 5 [curve (b) in both plots], where the quantity $2\cos^2\beta \mathrm{Im}Z_0$ is taken to be equal to one. We can appreciate from the plots that the net dependence on $m_H$ for this class of diagrams is rather weak and, as explained in the conclusions, this will probably cause important suppressions.

Moving on to class 4, we see that they are analogous to the diagrams studied by Barr and Zee [9] which give the dominant contributions to the EDM of the electron (and possibly the neutron) in this model. The contributions can be expressed, as in the class 3 case, in terms of $\mathrm{Im}Z_0$. The analytic expressions for the Feynman parameter integrals are relatively simple. For the diagram with a photon inside we have

$$f_\gamma(0) = \frac{e^2 g^2}{32\pi^4}(2\cos^2\beta \mathrm{Im}Z_0) F_{4,\gamma}(m_t, m_H) \ , \tag{30}$$

with the parametric integral given by

$$F_{4,\gamma}(m_t, m_H) = \frac{1}{3}\int_0^1 dw \int_0^1 dx \int_0^1 dy \int_0^1 dz x y^2 z \times [wyz + (m_W/m_t)^2(1-x)(1-y)^2 x + (m_H/m_t)^2(1-x)(1-w)xyz]^{-1} \ , \tag{31}$$

where the contributions from the unphysical Goldstone bosons have already been included. We still have to multiply the value of $f_\gamma(0)$ in (30) by 4, to take care of the symmetric diagrams. Doing so, and evaluating it for $m_t = 180$ GeV and $m_H = 100$ GeV we arrive at a total $f_\gamma(0)$ for this case of $-1.2 \times 10^{-5}\mathrm{Im}Z_0$. This is close to the contribution of diagram 1(a), assuming $\mathrm{Im}Z_0$ and $\mathrm{Im}Z_2$ to be comparable in magnitude.

In the case of an internal $Z^0$ boson (Fig. 4), only the vector part of the coupling of the $Z^0$ to the top-quark happens to contribute, but unlike the Barr-Zee case this does not entail a strong suppression relative to the photon diagram. This is because in the calculation of the electron EDM the coupling of the $Z^0$ to the electron is small, while in the case at hand the coupling is to the $W$ boson and the suppression factor is only about 65%. Consequently, these diagrams have to be included. Computing them, we find

$$f_\gamma(0) = \left(1 - \frac{1}{3}\tan^2\theta_W\right)\left(\frac{3}{8} - \sin^2\theta_W\right)\frac{g^4}{128\pi^4}(2\cos^2\beta \mathrm{Im}Z_0) F_{4,Z^0}(m_t, m_H) \ , \tag{32}$$

where the Feynman parameter integral is given by

$$F_{4,Z^0}(m_t, m_H) = \int_0^1 dw \int_0^1 dx \int_0^1 dy \int_0^1 dz x y^2 z [wyz + (m_W/m_t)^2(1-x)(1-y)^2 x + (m_H/m_t)^2(1-x)(1-w)xyz + (m_Z/m_t)^2(1-x)(1-z)xy]^{-1} \ . \tag{33}$$

This includes, as in the photon's case, the contributions from unphysical Goldstone bosons. Including symmetric diagrams (multiplying by 4) we get $f_\gamma(0) = -4.5 \times 10^{-6}\ \mathrm{Im}Z_0$, for $m_t = 180$ GeV and $m_H = 100$ GeV. As in the previous diagram the result is negative, but we need to keep in mind that we do not know the relative sign between $\mathrm{Im}Z_0$ and $\mathrm{Im}Z_2$ and so these results may add to or subtract from diagram 1(a). The EDM contributed by these diagrams (all of class 4) is shown in Fig. 5 [curve (c) in both plots], under the assumption $2\cos^2\beta \mathrm{Im}Z_0 = 1$.

## V. DISCUSSION AND CONCLUSIONS

We have computed the $W$ EDM in the two-Higgs-doublet extension of the SM. All the relevant diagrams have been included and the results are exhibited in Fig. 5, where the $CP$-violating quantities $\mathrm{Im}Z_2$ and $2\cos^2\beta \mathrm{Im}Z_0$ are set equal to one. We can see from the plot for $m_t = 180$ GeV, that a value for $d_W$ of about $5\times10^{-21} e$ cm can be easily achieved for relatively small masses of the dominant Higgs boson. This is below the current upper bound of $\sim 10^{-19} e$ cm, which comes indirectly from the experimental upper bound for the neutron EDM, $d_n = (-3 \pm 5) \times 10^{-26} e$ cm [10], after applying the Marciano-Queijeiro technique [5]. Nevertheless, this procedure involves the introduction of an ultraviolet cutoff and the corresponding bound may be misleading [11]. It also suffers from the well-known problems present in any calculation of the neutron EDM. To remedy part of these deficiencies, one of us (T.W.) undertook the exact calcu-

lation of the induced fermion EDM coming from the $W$ EDM in the minimal supersymmetric extension of the SM and in the two-Higgs-doublet extension of the SM [23]. In spite of being model dependent, these calculations eliminate the uncertainties involved in the use of cutoffs to regularize divergent integrals and provide a more secure footing for comparison with experiment. No constraints were found on the *CP*-violating phases in either theory.

Our results differ considerably from those of He and McKellar. For example, taking $m_t = 200$ GeV and $m_H = 100$ GeV, Eq. (4) of Ref. [12] yields $f_\gamma(0) = 2.7 \times 10{-}6$ (assuming their $\mathrm{Im}Z = 1$) for diagram 1(a). By contrast, we get $f_\gamma(0) = 1.8 \times 10^{-5}$ (with $\mathrm{Im}Z_2 = 1$) for the same diagram. After adding the contributions from the other diagrams (under the assumption that $\mathrm{Im}Z_2$ and $\mathrm{Im}Z_0$ are of opposite sign) our result is more than 10 times larger than that of Ref. [12]. (As noted in Sec. IV, He and McKellar now agree with us on the results for this diagram [14].)

Likewise, Vendramin [13] computed the $W$ EDM induced by the diagram of Fig. 1(a). For $m_t = 200$ GeV, $m_3 = 30$ GeV (corresponding to our dominant Higgs-boson mass $m_H$), $\tan\beta = 10$, $m_1 = 273$ GeV, and $m_2 = 187$ GeV [these are the other two neutral-Higgs-boson masses whose contributions we neglect in our calculations, computed from the parameters $\sin\xi = 0.6$ and $k = 2$ by means of Eq. (33), Ref. [13]], he finds (see Fig. 11 in Ref. [13]) $d_W \approx 10^{-20} e$ cm. The value we find for diagram 1(a), assuming $m_t = 200$ GeV and $m_H = 30$ GeV, is $d_W \approx 2.4 \times 10^{-21}\ \mathrm{Im}Z_2\, e$ cm. Taking the other two mass eigenstates into consideration should *reduce* this value (because of the sum rules we discuss below). On top of that, the choice $\tan\beta = 10$ implies an upper bound for $\mathrm{Im}Z_2$ of $\sim 10^{-1}$. The value we find is therefore 1 to 2 orders of magnitude *smaller* than Vendramin's, for this particular choice of parameters.

Chang *et al.* [15] also made a rough estimate of the $W$ EDM induced by Higgs exchange. Their inequality [Eq. (12) of Ref. [15]]

$$d_W \lesssim 10^{-20}(m_t/100\ \mathrm{GeV})^2(10\ \mathrm{GeV}/m_H)^2 e\,\mathrm{cm}\ , \quad (34)$$

yields, for $m_t = 180$ GeV and $m_H = 100$ GeV, a dipole moment $d_W \lesssim 3 \times 10^{-22} e$ cm which is roughly an order of magnitude smaller than what we get. For smaller Higgs boson masses the value is closer to ours. This is due, in part, to the inverse quadratic dependence on $m_H$ in their expression for $d_W$. Our results indicate a much milder dependence to the point of being almost disturbing, because the *CP*-violating amplitudes in the sums over mass eigenstates [Eqs. (10)–(13)] obey the sum rules [8]

$$\sum_n Z_{0,n} = \sum_n \tilde{Z}_{0,n} = \sum_n Z_{1,n} = \sum_n Z_{2,n} = 0 \quad (35)$$

that may be the cause of strong suppressions if the dependence on the neutral-Higgs-boson masses is too weak. Fortunately, for diagrams in classes 1 and 4 this will not appreciably affect our conclusions, as long as the Higgs-boson masses are well spaced. However, the contributions from class 3 diagrams will be highly suppressed if the mass of the lightest neutral Higgs boson is above $\sim 200$ GeV.

We know neither the magnitude nor the signs of the quantities $\mathrm{Im}Z_2$ and $\mathrm{Im}Z_0$. Nevertheless, for vacuum expectation values $\lambda_1$ and $\lambda_2$ of about the same size, the constraints found by Weinberg give for $|\mathrm{Im}Z_2|$ and $2\cos^2\beta|\mathrm{Im}Z_0|$ upper bounds of $\sqrt{2}$ and 1, respectively. No constraints come from the comparison of the dominant contributions to the EDM's of the electron and the neutron in this model [9] with the present experimental upper bounds; and the estimate $\tan\beta > 0.3$ made by Barger *et al.* [24] places no restrictions, either. So, we can assume $|\mathrm{Im}Z_2|$ and $2\cos^2\beta|\mathrm{Im}Z_0|$ to be of order unity (as we did for the graphs of Fig. 5). Of course, for values a little larger than one, the $W$ EDM could reach $10^{-20} e$ cm. However, for $|\lambda_2| \gg |\lambda_1|$ both upper bounds are much smaller than one and the contributions to the EDM will be strongly suppressed.

A $d_W \lesssim 10^{-20} e$ cm is too small to be seen at current accelerators. The form factor $f_\gamma(0)$, corresponding to this EDM, is $\sim 10^{-4}$. At the CERN $e^+e^-$ collider LEP II the sensitivity to this form factor may reach $10^{-1}$ and it is somewhat better at some proposed colliders such as the Next Linear Collider (NLC) [3,4]. Since good prospects exist for improvement of the EDM bounds for the electron and the neutron in the near future, the best chance of observing the consequences of a nonzero $W$ EDM is, for now, through the induced fermions EDM's.

## ACKNOWLEDGMENTS

We would like to thank U. van Kolck, who collaborated with us at the earliest stages of this work. One of us (R.L.M.) also thanks Siamak Gousheh for useful conversations. This work was supported in part by the Robert A. Welch Foundation and by the National Science Foundation under Grant No. PHY9009850.

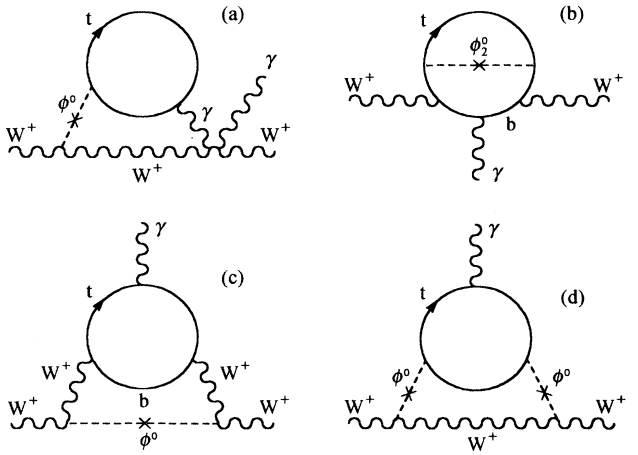


FIG. 7. A selection of a few *noncontributing* diagrams (for a discussion, see the Appendix). Many more could be added to this set.

## APPENDIX

As mentioned in Sec. III, there are many diagrams that do not generate contributions although they apparently possess all the necessary ingredients. For completeness, we give here a brief discussion of some representative diagrams.

The diagram of Fig. 7(a), and all other similar graphs with only two lines attached to the fermion loop, does not violate $P$ invariance. This is because the number of $\gamma$ matrices in the loop is insufficient to produce a Levi-Civita tensor. It therefore does not contribute to the EDM since we require *CP and P* violation.

Diagram 7(b) has a neutral Higgs propagator inside the fermion loop, reminiscent of class 1 diagrams in the notation of this paper. Still, there is no *CP* violation in this case because the final amplitude is proportional to $\mathrm{Re}Z_2$. An equivalent explanation would be to consider the effect of the neutral Higgs boson connected to the top quark. Since the photon is on the other side of the loop [see Fig. 7(b)] the presence of the Higgs boson amounts only to a correction of the self-energy of the virtual top, and this of course is *CP* invariant.

The case of Fig. 7(c) is somewhat analogous to the previous one. The amplitude for the diagram becomes proportional to $\mathrm{Re}Z_k$ (where $k$ depends on which neutral Higgs propagators are inserted) when the sum of the diagrams with a given Higgs propagator and its complex conjugate is performed.

Finally, Fig. 7(d) has *two* neutral Higgs bosons attached to the top quark. As happened for Fig. 7(a), there are not enough $\gamma$ matrices in the fermion loop to produce a Levi-Civita tensor. We could add many more diagrams to this list (for example, attaching the photon to different parts of the diagrams in Fig. 7), but in all cases the absence of contributions to the EDM of the $W$ boson is due to mechanisms analogous to the ones discussed.


[1] S. M. Barr and W. J. Marciano, in *CP Violation*, edited by C. Jarlskog (World Scientific, Singapore, 1989).

[2] W. Bernreuther and M. Suzuki, Rev. Mod. Phys. **63**, 313 (1991); X.-G. He, B. McKellar, and S. Pakvasa, Int. J. Mod. Phys. A **4**, 5011 (1989); see also Ref. [1].

[3] K. Hagiwara, R. D. Peccei, D. Zeppenfeld, and K. Hikasa, Nucl. Phys. **B282**, 253 (1987).

[4] A. Queijeiro, Phys. Lett. B **193**, 354 (1987); C. H. Chang and S. C. Lee, Phys. Rev. D **37**, 101 (1988); F. Boudjema, C. Hamzaoui, M. A. Samuel, and J. Woodside, Phys. Rev. Lett. **63**, 1906 (1989); G. Gounaris, D. Schildknecht, and F. M. Renard, Phys. Lett. B **263**, 291 (1991); A. Bilal, E. Masso, and A. De Rújula, Nucl. Phys. **B355**, 549 (1991).

[5] W. J. Marciano and A. Queijeiro, Phys. Rev. D **33**, 3449 (1986); F. Salzman and G. Salzmann, Phys. Lett. **15**, 91 (1965).

[6] M. J. Booth, Report No. EFI-93-01 (unpublished), and references therein. See also M. É. Pospelov and I. B. Khriplovich, Yad. Fiz. **53**, 1030 (1991) [Sov. J. Nucl. Phys. **53**, 638 (1991)].

[7] S. Weinberg, Phys. Rev. Lett. **63**, 2333 (1989).

[8] S. Weinberg, Phys. Rev. D **42**, 860 (1990).

[9] S. M. Barr and A. Zee, Phys. Rev. Lett. **65**, 21 (1990). See also R. G. Leigh, S. Paban, and R.-M. Xu, Nucl. Phys. **B352**, 45 (1991); J. F. Gunion and R. Vega, Phys. Lett. B **251**, (1990); D. Chang, W.-Y. Keung, and T. C. Yuan, Phys. Rev. D **43**, R14 (1991).

[10] K. F. Smith *et al.*, Phys. Lett. B **234**, 191 (1990).

[11] F. Boudjema, K. Hagiwara, C. Hamzaoui, and K. Numata, Phys. Rev. D **43**, 2223 (1991); see also Ref. [18].

[12] X.-G. He and B. McKellar, Phys. Rev. D **42**, 3221 (1990).

[13] I. Vendramin, Nuovo Cimento **106**, 79 (1993).

[14] X.-G. He (private communication); X.-G. He and B. McKellar, Phys. Rev. D **50**, 4719(E) (1994).

[15] D. Chang, W.-Y. Keung, and J. Liu, Nucl. Phys. **B355**, 295 (1991).

[16] L. D. Landau, Zh. Eksp. Teor. Fiz. **32**, 405 (1957) [Sov. Phys. JETP **5**, 336 (1957)]; E. M. Purcell and N. F. Ramsey, Phys. Rev. **78**, 807 (1950).

[17] J. F. Gaemers and G. Gounaris, Z. Phys. C **1**, 259 (1979); see also Ref. [3].

[18] D. Atwood, C. P. Burgess, C. Hamzaoui, B. Irwin, and J. A. Robinson, Phys. Rev. D **42**, 3770 (1990).

[19] J. F. Gunion, H. E. Haber, G. L. Kane, and S. Dawson, *The Higgs Hunter's Guide* (Addison-Wesley, Reading, MA, 1990), for a general survey.

[20] Wolfram Research Inc., MATHEMATICA V2.2. The standard reference is S. Wolfram, MATHEMATICA, *A System for Doing Mathematics by Computer*, 2nd ed. (Addison-Wesely, Redwood City, CA, 1991).

[21] T. West, Comput. Phys. Commun. **77**, 286 (1993); R. López-Mobilia (in preparation).

[22] C. P. Burgess (private communication).

[23] T. West, Phys. Rev. D **50**, 7025 (1994).

[24] V. Barger, J. L. Hewett, and R. J. N. Phillips, Phys. Rev. D **41**, 3421 (1990).